



TOWARDS AN UNBIASED DETERMINATION OF PARTON DISTRIBUTIONS WITH QED CORRECTIONS

Stefano Carrazza

On behalf of the NNPDF Collaboration

Dipartimento di Fisica, Università di Milano & INFN, Sezione di Milano

Via Celoria 16, I-20133 Milano, Italy

Electroweak corrections to hadron collider processes become relevant at the level of precision reached by present-day LHC experiments. We provide a preliminary discussion of the impact of electroweak corrections to parton distributions, concentrating on electrodynamic corrections to parton evolution equations, and showing a preliminary assessment of their impact. Furthermore, we determine the parton distribution function of the photon from deep inelastic scattering data using the NNPDF methodology.

Introduction The inclusion of quantum electrodynamics (QED) corrections to hadron collider processes, which in turns requires the determination of the photon parton distribution function (photon PDF) is motivated by the need for greater precision for LHC measurements, such as the W mass determination, high mass searches, WW production¹. Moreover, a precise determination of the photon PDF is needed for a reliable computation of several new physics signals, such as the cross-section for Z' and W' production.

Here we will include QED corrections up to leading order (LO) in $\mathcal{O}(\alpha)$, to next-to-leading order (NLO, i.e. $\mathcal{O}(\alpha_s^2)$) QCD computations. This choice is motivated by the similar magnitude of $\alpha_s^2(M_Z^2)$ and $\alpha(M_Z^2)$, which suggests that LO QED corrections and NLO QCD corrections are of a similar size.

Even though our final goal is the computation of LHC processes, we start by determining the impact of QED corrections and the photon PDF from deep-inelastic scattering (DIS). In such case, the photon PDF obtained is determined indirectly by DGLAP evolution, because at LO in QED there are no photon-induced processes in DIS. Consequently, we expect the uncertainties of the photon PDF determined from DIS to be large. Further information on the photon PDF can be obtained from collider processes to which the photon contributes at LO, such as vector boson production. While we will present a first assessment of the impact of QED corrections on these processes, their inclusion in the determination of the photon PDF will be presented elsewhere.

PDFs evolution The LO QED evolution equations^{2,3} which are coupled to the standard QCD DGLAP are

$$Q^2 \frac{\partial}{\partial Q^2} \gamma(x, Q^2) = \frac{\alpha(Q^2)}{2\pi} \left[P_{\gamma\gamma}(\xi) \otimes e_\Sigma^2 \gamma(z, Q^2) + P_{\gamma q}(\xi) \otimes \sum_j e_j^2 q_j(z, Q^2) \right], \quad (1)$$

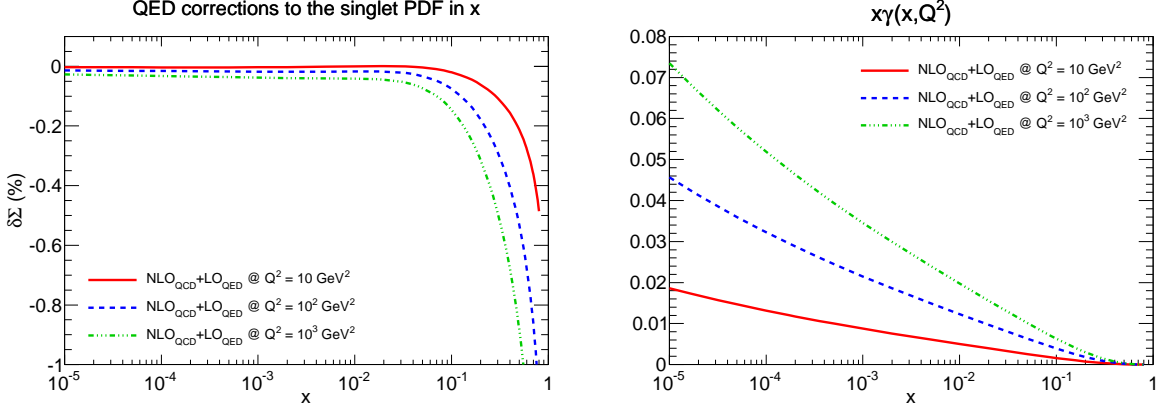


Figure 1: Impact of QED evolution on the singlet PDF, $\Sigma = \sum_i q_i$ when $\gamma(x, Q_0^2) = 0$ (left). The photon PDF generated dynamically at higher scales is shown on the right.

$$Q^2 \frac{\partial}{\partial Q^2} q_i(x, Q^2) = \frac{\alpha(Q^2)}{2\pi} \left[P_{q\gamma}(\xi) \otimes e_i^2 \gamma(z, Q^2) + P_{qq}(\xi) \otimes e_i^2 q_i(z, Q^2) \right], \quad (2)$$

where $\gamma(x, Q^2)$ and $q_i(x, Q^2)$ are respectively the PDF of the photon and the i -th quark flavor, $P_{ij}(\xi)$ are splitting functions, e_i the quark electric charge, and $e_\Sigma^2 = N_c \sum_i e_i^2$ the sum over all active quark flavors with $N_c = 3$. When combining QCD and QED evolution, PDFs satisfy the momentum sum rule

$$\int_0^1 dx x \left\{ \sum_i q_i(x, Q^2) + g(x, Q^2) + \gamma(x, Q^2) \right\} = 1. \quad (3)$$

There are several methods to solve the combined QCD+QED DGLAP evolution equations, for example by finding a PDF basis which simultaneously diagonalizes the system as in Ref. ². We have developed a combined solution which optimizes the matching to the NNPDF implementation.

The effect of QED evolution on the singlet PDF is shown in the left plot of Figure 1, where the percentage correction to NLO QCD DGLAP evolution due to the inclusion of QED is shown for different scales Q^2 , using as input the `Les Houches toy PDF` ⁴ and setting $\gamma(x, Q_0^2) = 0$ at the initial scale $Q_0^2 = 2 \text{ GeV}^2$. We observe differences of the permille level at large- x , though effects are more pronounced at higher energies: LO QED corrections due to evolution are small, however the initial photon PDF has been so far assumed to vanish. The right plot of Figure 1 shows the photon PDF generated dynamically at energies above the initial scale $Q^2 > 2 \text{ GeV}^2$.

Photon PDF from DIS data With QED corrections to DIS included up to LO through QED evolution, we can now try to determine the photon PDF from a fit to DIS data. We use the DIS dataset included in the NNPDF2.3 ⁵ determination, shown in the (x, Q^2) plane in Figure 2, which includes 2767 data points.

A consequence of the inclusion of QED corrections is isospin symmetry breaking: the neutron PDFs cannot no longer be obtained from the proton PDFs using isospin, i.e. $u^n \neq d^p$, $d^n \neq u^p$. However, we assume that isospin holds at the starting scale Q_0^2 . It is then broken dynamically by DGLAP evolution.

In the NNPDF framework ^{5,6}, we generate a set of Monte Carlo replicas of the data, then from each replica we extract a PDF set. The minimization is performed by a genetic algorithm and the best fit is determined by cross-validation. One of the most important advantages of this methodology is that it minimizes the bias related to the choice of functional form of PDFs. We parametrize the photon PDF, like all other PDFs, with a feed-forward neural network with

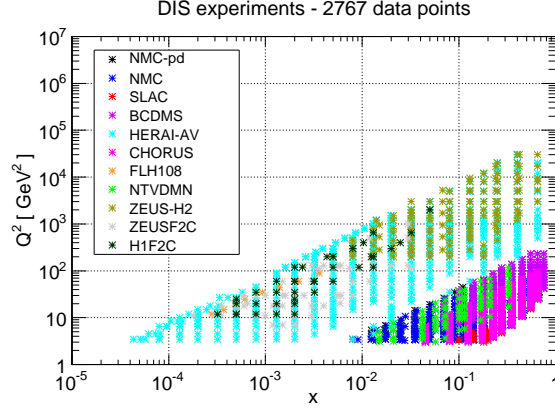


Figure 2: Kinematic coverage of the experimental DIS data used in the determination of the photon PDF.

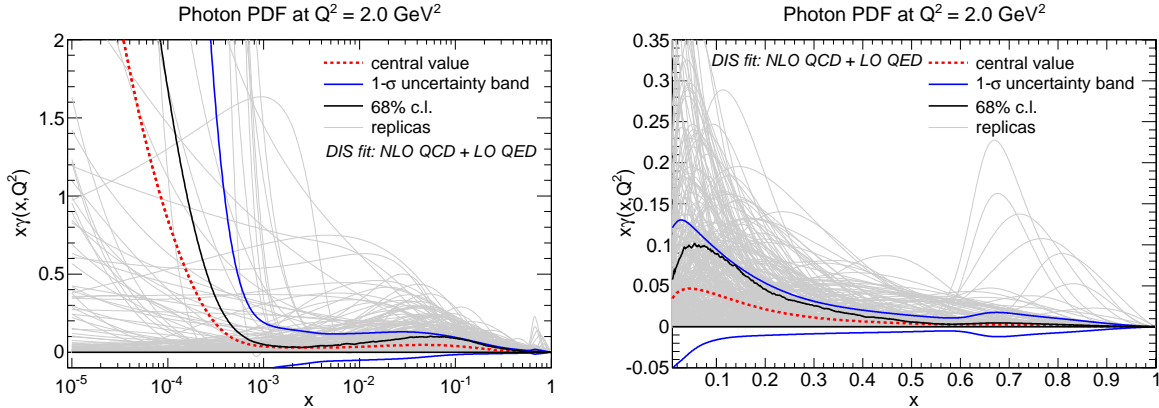


Figure 3: The photon PDF extracted from DIS data, NLO QCD + LO QED, at $Q^2 = 2 \text{ GeV}^2$. The Monte Carlo PDF set includes 500 replicas.

2-5-3-1 architecture, which corresponds to a total of 37 parameters to be determined during the minimization procedure. Positivity of the photon PDF at LO is imposed by squaring the output of the neural network. The rest of the procedure is the standard NNPDF one.

The photon PDF from DIS is showed in Figure 3, in logarithmic (left) and linear (right) scales. The plots show the central value, the $1\text{-}\sigma$ and 68% c.l. uncertainties bands, and the 500 PDF replicas. The photon from DIS data is compatible with zero with large uncertainties. The photon PDF is less uncertain at central and large- x than at small- x , due to the lack of data points in this region (see Figure 2). The overall fit quality, as measured by the total χ^2 per data point, is $\chi^2 = 1.10$.

The impact of the photon PDF from DIS In order to understand the impact and the quality of the photon PDF just presented, we have computed $Z \rightarrow \mu^+\mu^-$ production in proton-proton collision at $\sqrt{s} = 14 \text{ TeV}$ with $|\eta^l| \leq 2.5$ and $p_T^l \geq 20 \text{ GeV}$ using HORACE⁷, which is a Monte Carlo event generator for Drell-Yan processes including the exact 1-loop electroweak radiative corrections $\mathcal{O}(\alpha)$. HORACE also provides the possibility to complement the $\mathcal{O}(\alpha)$ with photon initiated (photon-induced) processes at Born and NLO levels. The Born photon-induced contribution must be included at the order at which we are working. We have also included the NLO corrections, which however have a very small effect.

Figure 4 shows the Z invariant mass and the lepton p_T^l distributions, for 100 replicas and using the 68% c.l. uncertainty band. There is a moderate relative difference between $\mathcal{O}(\alpha)$

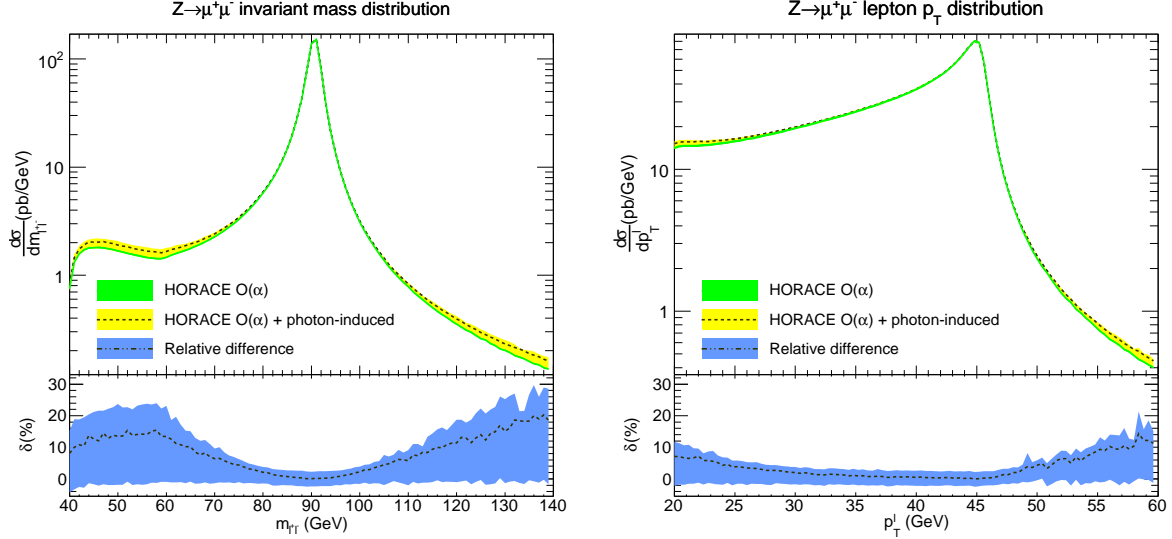


Figure 4: Z invariant mass and lepton p_T^l distribution computed using HORACE at $\sqrt{s} = 14$ TeV, with $|\eta^l| \leq 2.5$ and $p_T^l \geq 20$ GeV. Results to $\mathcal{O}(\alpha)$ with and without photon-induced contributions are compared.

and $\mathcal{O}(\alpha) +$ photon-induced processes due to the photon PDF, in the region of the m_{ll} and p_T^l peaks, which rapidly increases when going away from the respective peaks. The increase of the central value is expected, in fact, for example at the Born level we are adding the $\gamma\gamma \rightarrow \mu^+\mu^-$ processes to the usual $q\bar{q} \rightarrow \mu^+\mu^-$, however also the uncertainties grow when going far from the peak region. These large uncertainties reflect the uncertainty in the photon PDF, which is insufficiently constrained by DIS data.

Outlook Our results show that the photon PDF is only poorly constrained by DIS data, especially at small- x . Corrections to Z production due to photon-induced processes in the presence of such a large unconstrained PDF off the peak become rapidly larger than the data allow. This suggests that these and similar data should be used to determine the photon PDF itself. This determination will be presented elsewhere.

References

1. G. Bozzi, J. Rojo and A. Vicini, Phys. Rev. D **83** (2011) 113008 [arXiv:1104.2056 [hep-ph]].
2. M. Roth and S. Weinzierl, Phys. Lett. B **590** (2004) 190 [hep-ph/0403200].
3. A. D. Martin, R. G. Roberts, W. J. Stirling and R. S. Thorne, Eur. Phys. J. C **39** (2005) 155 [hep-ph/0411040].
4. W. Giele, E. W. N. Glover, I. Hinchliffe, J. Huston, E. Laenen, E. Pilon, A. Vogt and S. Alekhin *et al.*, hep-ph/0204316.
5. R. D. Ball, V. Bertone, S. Carrazza, C. S. Deans, L. Del Debbio, S. Forte, A. Guffanti and N. P. Hartland *et al.*, Nucl. Phys. B **867** (2013) 244 [arXiv:1207.1303 [hep-ph]].
6. R. D. Ball *et al.* [NNPDF Collaboration], Nucl. Phys. B **855** (2012) 153 [arXiv:1107.2652 [hep-ph]].
7. C. M. Carloni Calame, G. Montagna, O. Nicrosini and A. Vicini, JHEP **0710** (2007) 109 [arXiv:0710.1722 [hep-ph]].